KJVR
Korean Journal of Veterinary Research

Original Article

pISSN 2466-1384 · eISSN 2466-1392
Korean J Vet Res 2023;63(3):e26
https://doi.org/10.14405/kjvr.20230030

*Corresponding author:
Young-Won Lee
College of Veterinary Medicine and Research Institute of Veterinary Medicine, Chungnam National University, 99 Daehak-ro, Yuseong-gu, Daejeon 34134, Korea
Tel: +82-42-821-6786
E-mail: lywon@cnu.ac.kr
https://orcid.org/0000-0003-3207-0989

Conflict of interest:
The authors declare no conflict of interest.

Received: Jul 27, 2023
Revised: Aug 17, 2023
Accepted: Aug 28, 2023

Magnetic resonance imaging features of syringobulbia in small breed dogs

Young-Mok Song[1], In Lee[2], Yu-Mi Song[2], Ho-Jung Choi[1], Young-Won Lee[1,*]

[1]College of Veterinary Medicine and Research Institute of Veterinary Medicine, Chungnam National University, Daejeon 34134, Korea
[2]Ian Animal Diagnostic Center, Seoul 06014, Korea

Abstract

Syringobulbia is a rare neurological disorder characterized by a fluid-filled cavity in the brainstem. In this study, clinical signs, features on magnetic resonance imaging (MRI), and the diseases present concurrently with syringobulbia were investigated in 33 small breed dogs. Most dogs (97%) had concurrent syringomyelia, and some dogs (24%) presented with vestibular or cranial nerve symptoms associated with the medulla oblongata. MRIs revealed slit-like, bulbous, and vertical linear shapes of the cavities on T2-weighted hyperintense and T1-weighted hypointense signals similar to the cerebrospinal fluid. Chiari-like malformations were identified in all dogs. This study highlights the association of syringobulbia with syringomyelia and Chiari-like malformations in small breed dogs with or without brainstem-associated clinical signs.

Keywords: dogs; magnetic resonance imaging; medulla oblongata; syringomyelia; cerebellum

Introduction

Syringobulbia is a neurological disorder characterized by a fluid-filled cavity within the brainstem. It is a very rare condition in humans and animals [1,2]. The causes of syringobulbia in humans include hindbrain abnormalities, such as type 1 and type 2 Chiari malformations, tumors, trauma, meningitis, and hemorrhage [3–8]. This condition may also occur in an isolated form. The cavitary lesions are mainly located in the medulla but may extend to the pons, midbrain, and cerebrum [9,10].

In humans, syringobulbia can be classified into 2 types: communicating and noncommunicating. The communicating type is characterized by an increase in cerebrospinal fluid (CSF) pressure in the fourth ventricle, which may extend to involve the medulla. The noncommunicating type arises from disturbances in the flow of CSF [6,11,12]. In humans, patients with syringobulbia display gradual and progressive clinical signs, depending on the location of the cavity, damaged nerve cells, and subsequent gliosis [3,5,13]. The clinical signs of syringobulbia can vary from severe respiratory symptoms to mild signs of cranial nerve injury. Subclinical syringobulbia has also been reported [5,14].

In veterinary medicine, there is a solitary study describing the clinical signs and magnetic resonance imaging (MRI) features of syringobulbia in 8 dogs [1]. This report demonstrated that clinical signs and symptoms of syringobulbia in dogs include vestibular symptoms and sensory deficits, as well as differences in the shapes

of the syringobulbia. This previous study has some limitations, including the small number of dogs included in the study and the fact that half of them were from a single breed, Cavalier King Charles Spaniel. Therefore, the current study was performed to investigate clinical signs, MRI features, and concurrent diseases in cases of syringobulbia in a larger number of dogs from different breeds.

Materials and Methods

This retrospective study reviewed clinical and imaging data from 3 institutions (Chungnam National University Hospital, Daekyung Animal Imaging Center, and Ian Animal Medical Center, Korea) from August 2015 to September 2019 to identify dogs diagnosed with syringobulbia based on their brain MRIs. The inclusion criteria were dogs with a complete medical record (signalments, clinical signs, results of neurological examination, and blood test results) and CSF-like signals in the brainstem on the T1- and T2-weighted transverse and sagittal images of MRI from the midbrain to the medulla oblongata. If available, fluid-attenuated inversion recovery (FLAIR) images were additionally evaluated.

The breed, age, sex, and body weight of the selected dogs were analyzed. The clinical signs and symptoms were analyzed and classified based on their medical history and the results of the neurological examinations.

MRI was performed at 3 hospitals with 3 different 1.5T MR systems (Vantage Elan, Cannon Medical Systems Co., Ltd., Japan; Vantage Exerlert, Cannon Medical Systems Co., Ltd., Japan; Magnesium Essenza, Siemens Healthineers Co., Ltd., Germany). T2-weighted (TR 2950-6400 ms, TE 76–90 ms), T1-weighted (TR 450–725 ms, TE 14–17 ms), and FLAIR (TR 6900-9000 ms, TE 69–78 ms) images of the transverse and sagittal sections were scanned with a slice thickness of 2.5 to 3 mm. These MR images were evaluated with a commercially available picture archiving communication system (PACS Zetta; TY Soft Co., Ltd., Korea).

The MRI signals of the cavities in the medulla oblongata were classified into hyperintense, isointense, and hypointense and into slit-like, bulbous, vertical, and linear types depending on the shape of the cavities (Fig. 1). In addition, the location and number of cavities were also assessed.

The concurrent presence of syringomyelia, ventricular dilatation, Chiari-like malformations, dorsal atlantoaxial bands, atlantoaxial instability, atlanto-occipital overlapping, medullary kinking, and arachnoid cysts was evaluated. If possible, the severity of the concurrent diseases was also evaluated. The syringomyelia was assessed on the T2-weighted transverse images of the cervical spinal cord. The ratio of heights of the syrinx to the spinal cord at the most severe level was recorded. If the ratio was less than 0.33, it was set to grade 1; 0.33 or greater but less than 0.6, was set to grade 2; 0.6 or greater, was set to grade 3 [15]. Ventricular dilatation was expressed by measuring the height ratios of the ventricles and brain parallel to the falx cerebri on the T1-weighted transverse images at the interthalamic adhesion. If the ratio was less than 0.22, it was set to grade 0; 0.22 or greater but less than 0.7, was set to grade 1; greater than or equal to 0.7, was set to grade 3 [1]. Chiari-like malformations were assessed for the cerebellar shape, cerebellar hernia, and caudoventral cerebellar subarachnoid signal on the T2-weight-

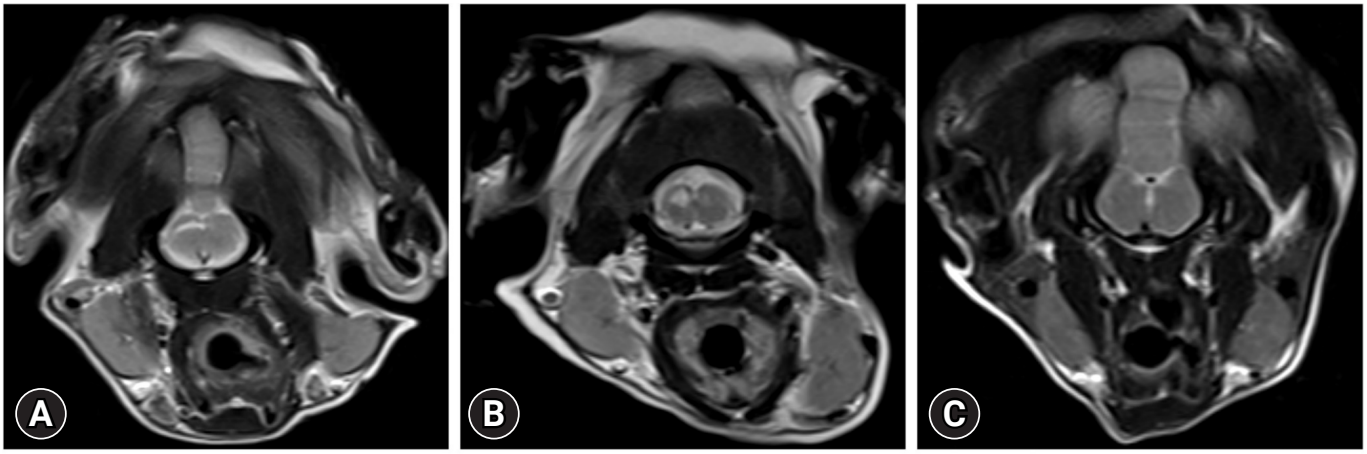

Fig. 1. Transverse T2-weighted images on magnetic resonance imaging of the caudal brainstem. Note the 3 shapes of syringobulbia including slit-like (A), bulbous (B), and vertical linear (C).

https://doi.org/10.14405/kjvr.20230030

ed mid-sagittal images [16–19]. Grade 0 was defined as the normal cerebellum; grade 1 as the cerebellum with deformities but no hernias; grade 2 as the cerebellum with a hernia in the direction of the foramen magnum [20]. Atlanto-occipital overlapping was evaluated on the T1-weighted sagittal images. Grade 0 was set if the dorsocranial lamina of the atlas did not touch the extended imaginary line connecting the caudodistal side of the supraoccipital bone with the posterior end of the basioccipital bone; grade 1 if it reached the line, and grade 2 if the anterior side was observed beyond the line [20]. The atlantoaxial band was assessed on T2-weighted sagittal images [21]. The atlantoaxial instability, medullary kinking, and arachnoid cyst were assessed on T1-weighted sagittal images [15,21–23].

Results

Thirty-three dogs met the inclusion criteria, with a median age of 5 years (range, 8 months to 15 years) and a median body weight of 2.5 kg (range, 1.7 kg to 4.7 kg). The breeds included 23 Maltese, 3 Pomeranians, 3 Chihuahuas, and one each of Toy Poodle, Miniature Pinscher, Yorkshire Terrier, and mixed breed dogs. There were 15 spayed females, 9 intact females, 6 castrated males, and 3 intact males.

Clinical signs and symptoms included ataxia, generalized seizure, head tilt, head turn, generalized tremor, nystagmus, sensory deficit, dysphagia, circling, and neck pain (Table 1). Seven dogs showed vestibular symptoms of head tilt, nystagmus, and circling, and one dog showed dysphagia suspected to be due to cranial nerve injury. Thus, 8 dogs had vestibular or cranial nerve signs associated with the medulla oblongata.

A total of 35 cavities were observed on the MRI of 33 dogs because multiple lesions were present in 2 dogs. The cavities were hyperintense on the T2-weighted images and hypointense on the T1-weighted images, consistent with the CSF signals (Fig. 2). Two dogs did not undergo FLAIR imaging. On the FLAIR images of the remaining 31 dogs, the lesions in 27 dogs showed hypointense signal intensity, 3 hyperintense, and one isointense. The shape of the syrinx was slit-like in 20 dogs, bulbous in 12 dogs, and vertical linear in 3 dogs. All the cavities were located in the medulla oblongata, with 14 lesions on the left side, 17 on the right, and 4 in the middle.

Syringomyelia was identified in 32 (97.1%) dogs, including grade 3 in 24 dogs, grade 2 in 7 dogs, and grade 1 in one dog. Ventricular dilatation was observed in 28 out of 33 (84.8%)

Table 1. Clinical signs and symptoms of dogs with syringobulbia

Clinical sings	No. of dogs
Brain stem	
Head tilt	4
Nystagmus	2
Circling	1
Dysphagia	1
Forebrain	
Seizure	15
Head turn	3
Others	
Ataxia	16
Tremor	3
Neck pain	1

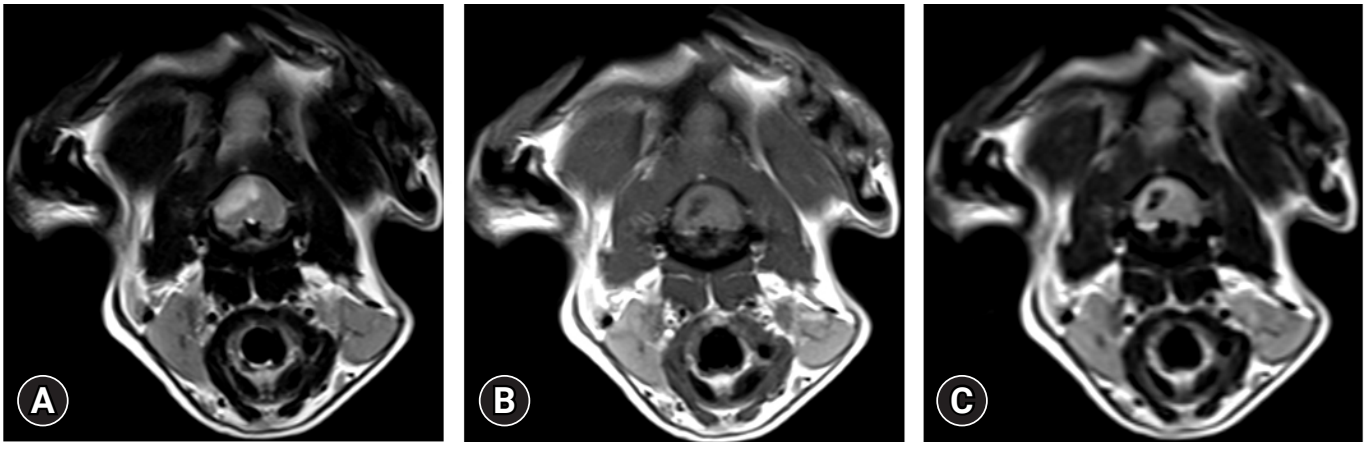

Fig. 2. Transverse T2-weighted (A), T1-weighted (B), and fluid-attenuated inversion recovery (FLAIR) (C) images of the medulla oblongata on magnetic resonance imaging (MRI) in a 9-year-old intact male Maltese (A-C). Note that the bulbous-shaped syrinx in the medulla oblongata, and similar signal intensity to cerebrospinal fluid (hyperintense in T2-weighted image, and hypointense in T1-weighted and FLAIR images).

dogs, all of which were grade 1. Chiari-like malformations were observed in all dogs, including grade 1 in 15 dogs and grade 2 in 18 dogs. Atlantoaxial overlapping was observed in 14 dogs (42.4%), of which 10 dogs were grade 1, and 4 dogs were grade 2. Dorsal atlantoaxial bands were found in 24 dogs (72.7%), medullary kinking in 12 dogs (36.4%), and arachnoid cysts in 18 dogs (54.5%). Atlantoaxial instability was not observed.

Discussion

A previous and sole study on this subject described the clinical and imaging features of syringobulbia in 8 dogs [1]. All the dogs in this study had concomitant syringomyelia. The present study investigated syringobulbia in a larger cohort of 33 small breed dogs, and like the previous study, most dogs (97.1%) had syringomyelia, but some did not. This is believed to be due to one of the causes for both conditions, namely, the disturbance of CSF flow, or the breed predilection for the craniocervical junction abnormalities.

In the present study, 8 of the 33 dogs (24.2%) had vestibular or cranial neurological symptoms associated with the medulla oblongata. Thus, it was different from the previous study, in which all dogs with syringobulbia had vestibular or cranial nerve signs [1]. In humans, symptomatic syringobulbia may also be characterized by headaches, vertigo, voice disturbances, paresthesia, dysphagia, tinnitus, hearing difficulty, nystagmus, ptosis, diplopia, palatal palsy, accessory nerve palsy, hypoglossal palsy, oculomotor palsy, etc. Respiratory disturbance has also been reported with syringobulbia. However, there have also been reports of patients with syringobulbia without any clinical signs [3,9,10,13,14,24].

On MRI, the cavities in the medulla oblongata showed CSF signals on the T2- and T1-weighted images and 3 dogs showed hyperintensities while one showed isointensity on FLAIR. This may be due to a limitation of the MRI resolution because the size of the most common slit-like type is very small. FLAIR imaging is generally not the first sequence necessary for the diagnosis of syrinx and is used to identify periventricular edema in cases of acute hydrocephalus and to exclude inflammatory diseases while diagnosing syrinx [25]. However, studies have found that intra-tumoral cavities and post-traumatic chronic lesions, the underlying mechanism of cavities in the medulla oblongata of humans, were irrelevant to CSF, and the features of these cavities were not identical to CSF; a veterinary study has also reported similar results of chronic lesions after trauma within the spinal cord [26]. Therefore, the FLAIR sequence can also help identify the causative diseases of cavities in dogs. In humans, syringobulbia has been reported to be well observed on T1-weighted images as well as on T2-weighted images [2]. In this study, as the most common slit-like form was thin, it was more difficult to identify syringobulbia on T1-weighted and FLAIR images compared to T2-weighted images. This was believed to be due to the MRI resolution, and because this type was spread outward from the center, it was best evaluated in the transverse T2-weighted images.

In addition to the slit-like and bulbous-shaped cavities that had been reported in the earlier study in dogs [1], this study also found a vertical linear shape in 3 dogs. This type could be a new form of syringobulbia or it may be a preceding stage to the slit-like or bulbous type. This is because, in the previous study, a bulbous type syringobulbia in a dog had increased in size on subsequent MRIs [1]. Further research is required to determine the clinical presentation and progression of the vertical linear type syringobulbia.

In humans, the causative diseases of syringobulbia are hindbrain abnormalities such as type 1 Chiari malformations, tumors, inflammatory diseases, and trauma [4]. Among these, syringobulbia is mainly caused by a hindbrain abnormality associated with the blockage of CSF flow [4]. In this study, all the dogs with syringobulbia were identified with a Chiari-like malformation, and 97.0% of the dogs had syringomyelia. Chiari-like malformations result from a condition where the caudal fossa is smaller than the size of the hindbrain. This condition narrows the foramen magnum, resulting in disruptions to the flow of CSF, thus causing cervical syringomyelia [16–19,25].

This study has some limitations. Of the 2 male dogs out of the 8 with vestibular or cranial nerve signs associated with medulla oblongata, one had meningoencephalitis of an unknown etiology and the other had moderate hydrocephalus. Therefore, we could not completely exclude the possibility that causes other than syringobulbia generated the clinical signs. Moreover, a histopathological examination of the syrinx was not performed.

In conclusion, syringobulbia was observed in small breed dogs and was found to be slit-like, bulbous, and of the vertical linear type in the medulla oblongata. It did not necessarily accompany the clinical signs associated with brainstem abnormalities and may also be closely associated with syringomyelia and Chiari-like malformations.

ORCID

Young-Mok Song, https://orcid.org/0000-0002-2247-5694
In Lee, https://orcid.org/0009-0000-8079-2332

https://doi.org/10.14405/kjvr.20230030

Yu-Mi Song, https://orcid.org/0009-0007-4773-1360
Ho-Jung Choi, https://orcid.org/0000-0001-7167-0755
Young-Won Lee, https://orcid.org/0000-0003-3207-0989

References

1. Williamson B, Davies E, Epperly E, Roynard P, Scrivani PV. Signs consistent with syringobulbia may be detected in dogs undergoing MRI. Vet Radiol Ultrasound 2019;60:390–399.
2. Sherman JL, Citrin CM, Barkovich AJ. MR imaging of syringobulbia. J Comput Assist Tomogr 1987;11:407–411.
3. Jha S, Das A, Gupta S, Banerji D. Syringomyelia with syringobulbia presenting only with paralysis of 9th and 10th cranial nerves. Acta Neurol Scand 2002;105:341–343.
4. Menezes AH, Greenlee JD, Dlouhy BJ. Syringobulbia in pediatric patients with Chiari malformation type I. J Neurosurg Pediatr 2018;22:52–60.
5. Taghipour M, Derakhshan N, Ghaffarpasand F. Isolated post-traumatic syringobulbia; case report and review of the literature. Bull Emerg Trauma 2014;2:166–169.
6. Mousele C, Georgiopoulos M, Constantoyannis C. Syringobulbia: a delayed complication following spinal cord injury: case report. J Spinal Cord Med 2019;42:260–264.
7. Shen J, Shen J, Huang K, Wu Y, Pan J, Zhan R. Syringobulbia in patients with Chiari malformation type I: a systematic review. Biomed Res Int 2019;2019:4829102.
8. Shuster A, Landry D. Case 191: giant hemorrhagic syringomyelia and syringobulbia mimicking intramedullary neoplasm. Radiology 2013;266:991–993.
9. Greenlee JD, Menezes AH, Bertoglio BA, Donovan KA. Syringobulbia in a pediatric population. Neurosurgery 2005;57:1147–1153.
10. Menezes AH, Greenlee JD, Longmuir RA, Hansen DR, Abode-Iyamah K. Syringohydromyelia in association with syringobulbia and syringocephaly: case report. J Neurosurg Pediatr 2015;15:657–661.
11. Milhorat TH. Classification of syringomyelia. Neurosurg Focus 2000;8:E1.
12. Nogués M, López L, Meli F. Neuro-ophthalmologic complications of syringobulbia. Curr Neurol Neurosci Rep 2010;10:459–466.
13. Gennaro P, Miller M. Syringobulbia without syringomyelia. Arch Neurol 1983;40:394.
14. Nogués M, Gené R, Benarroch E, Leiguarda R, Calderón C, Encabo H. Respiratory disturbances during sleep in syringomyelia and syringobulbia. Neurology 1999;52:1777–1783.
15. Cerda-Gonzalez S, Olby NJ, Griffith EH. Medullary position at the craniocervical junction in mature cavalier King Charles spaniels: relationship with neurologic signs and syringomyelia. J Vet Intern Med 2015;29:882–886.
16. Driver CJ, Volk HA, Rusbridge C, Van Ham LM. An update on the pathogenesis of syringomyelia secondary to Chiari-like malformations in dogs. Vet J 2013;198:551–559.
17. Knowler SP, Galea GL, Rusbridge C. Morphogenesis of canine Chiari malformation and secondary syringomyelia: disorders of cerebrospinal fluid circulation. Front Vet Sci 2018;5:171.
18. Marino DJ, Loughin CA, Dewey CW, Marino LJ, Sackman JJ, Lesser ML, Akerman MB. Morphometric features of the craniocervical junction region in dogs with suspected Chiari-like malformation determined by combined use of magnetic resonance imaging and computed tomography. Am J Vet Res 2012;73:105–111.
19. Rusbridge C. Chiari-like malformation and syringomyelia. Eur J Companion Anim Pract 2013;23:70–89.
20. Kiviranta AM, Rusbridge C, Laitinen-Vapaavuori O, Hielm-Björkman A, Lappalainen AK, Knowler SP, Jokinen TS. Syringomyelia and craniocervical junction abnormalities in Chihuahuas. J Vet Intern Med 2017;31:1771–1781.
21. Cerda-Gonzalez S, Olby NJ, Griffith EH. Dorsal compressive atlantoaxial bands and the craniocervical junction syndrome: association with clinical signs and syringomyelia in mature cavalier King Charles spaniels. J Vet Intern Med 2015;29:887–892.
22. Takahashi F, Kouno S, Yamaguchi S, Hara Y. Evaluation of atlantooccipital overlapping and cerebral ventricle size in dogs with atlantoaxial instability. J Vet Med Sci 2019;81:229–236.
23. Matiasek LA, Platt SR, Shaw S, Dennis R. Clinical and magnetic resonance imaging characteristics of quadrigeminal cysts in dogs. J Vet Intern Med 2007;21:1021–1026.
24. Morgan D, Williams B. Syringobulbia: a surgical appraisal. J Neurol Neurosurg Psychiatry 1992;55:1132–1141.
25. Rusbridge C, Stringer F, Knowler SP. Clinical application of diagnostic imaging of Chiari-like malformation and syringomyelia. Front Vet Sci 2018;5:280.
26. Alisauskaite N, Spitzbarth I, Baumgärtner W, Dziallas P, Kramer S, Dening R, Stein VM, Tipold A. Chronic post-traumatic intramedullary lesions in dogs, a translational model. PLoS One 2017;12:e0187746.